Carbohydrate Polymers 97 (2013) 269–276

Contents lists available at SciVerse ScienceDirect

Carbohydrate Polymers

journal homepage: www.elsevier.com/locate/carbpol

Fracture behavior of a commercial starch/polycaprolactone blend reinforced with different layered silicates

E. Pérez [a], C.J. Pérez [b], V.A. Alvarez [c], C. Bernal [a,*]

[a] INTECIN (UBA-CONICET), Engineering Faculty, University of Buenos Aires, Av. Las Heras 2214, C1127AAR Buenos Aires, Argentina
[b] Polymer Science and Engineering Group, Materials Science and Technology Research Institute (INTEMA), National University of Mar del Plata-National Research Council (CONICET), Av. Juan B. Justo 4302, B7608FDQ Mar del Plata, Argentina
[c] Composite Materials Group (CoMP), Materials Science and Technology Research Institute (INTEMA), National University of Mar del Plata-National Research Council (CONICET), Av. Juan B. Justo 4302, B7608FDQ Mar del Plata, Argentina

ARTICLE INFO

Article history:
Received 20 February 2013
Received in revised form 29 April 2013
Accepted 30 April 2013
Available online xxx

Keywords:
Fracture toughness
Failure
Biodegradable composites
Clay

ABSTRACT

In the present work, composites based on a commercial starch/PCL blend (MaterBi-Z) reinforced with three different nanoclays: natural montmorillonite (Cloisite Na^+ (MMT)) and two modified montmorillonites (Cloisite 30B (C30B) and Cloisite 10A (C10A)) were prepared in an intensive mixer. The aim of this investigation was to determine the effect of the different nanoclays on the quasi-static fracture behavior of MaterBi-Z nanocomposites. An improvement in the fracture behavior for the composite with low contents of C30B was obtained, probably due to the easy debonding of clay achieved from a relatively weak filler–matrix interaction. On the other hand, a strong interaction had a detrimental effect on the material fracture toughness for the MaterBi-Z/C10A composites as a result of the higher compatibility of this organo-modified clay with the hydrophobic matrix. Intermediate values of fracture toughness, determined using the *J*-integral approach (J_c), were found for the composites with MMT due to its intermediate interaction with the matrix. The different filler–matrix interactions observed were also confirmed from the application of Pukánszky and Maurer model. In addition, multifractal analysis was applied to describe the topography of fracture surfaces. Thus, the complex fracture process could be successfully described by both experimental and theoretical tools. The obtained results suggest that it is possible to tailor the mechanical properties of the studied composites taking into account their further application.

1. Introduction

Over the recent decades, biodegradable polymers have been extensively investigated for packaging and agricultural applications to reduce the environmental pollution caused by plastic wastes (Davis & Song, 2006; Scott, 2000; Siracusa, Rocculi, Romani, & Dalla Rosa, 2008). In order to compete with common synthetic plastics, biodegradable polymers must have low cost as well as comparable mechanical properties. Starch-based blends present an enormous potential to be widely used in the field of biomedical applications and environmentally friendly materials, as they are fully biodegradable, inexpensive (when compared to other biodegradable polymers) and available in large quantities (Chen & Evans, 2005; Sorrentino, Gorrasi, & Vittoria, 2007). Blends of gelatinized starch with biodegradable polymers such as polyhydroxybutyrate (PHB) or polycaprolactone (PCL) have been studied by many authors (Godbole, Gote, Latkar, & Chakrabarti, 2003; Corradini, Marconcini, Agnelli, & Mattoso, 2011; Reis et al., 2008; Rosa, Lopes, & Calil, 2005; Wu, 2003).

Particularly, blends of poly-ε-caprolactone (PCL) and starch were introduced into the market at the beginning of the 90s as packaging materials (Ishiaku, Pang, Lee, & Ishak, 2002; Siracusa et al., 2008). It has been shown that physical and mechanical properties of these blends are similar to those of some conventional plastics, but they have the advantage of being biodegradable in different environments (Corradini et al., 2011; Reis et al., 2008; Rosa et al., 2005).

In addition, it has been well established in the literature that the incorporation of inorganic fillers is also a possible way to improve mechanical properties of polymeric materials (Xu, Li, Heng, & Mai, 2006). Starch/PCL blends based composites have been extensively investigated (Chen & Evans, 2005; Vertuccio, Gorrasi, & Sorrentino, 2009; Zhang, Yu, Xie, Naito, & Kagawa, 2007). In previous works, the creep behavior, the tensile properties as well as the effect of water uptake on these properties for starch/PCL blends reinforced with different types of clays have been already analyzed (Pérez, Alvarez, Mondragón, & Vázquez, 2007; Pérez, Alvarez, & Vázquez,

* Corresponding author. Tel.: +54 11 43430891/2775x381/388; fax: +54 11 43457562.
E-mail addresses: cbernal@fi.uba.ar, japerez1970@hotmail.com (C. Bernal).

0144-8617/$ – see front matter © 2013 Elsevier Ltd. All rights reserved.
http://dx.doi.org/10.1016/j.carbpol.2013.04.099

2008; Pérez, Alvarez, Mondragón, & Vázquez, 2008). Besides, the influence of the content and type of clay on the dynamic and isothermal crystallization behavior of these materials has been reported (Pérez & Alvarez, 2008; Pérez, Alvarez, Stefani, & Vázquez, 2006).

Although many works have been already published on biodegradable materials, as mentioned above, in order to extend the applications of this kind of polymers, its blends and composites, the tensile, fracture, impact and damage behavior should be analyzed. Elucidation of the different toughening mechanisms present in these materials should also be investigated. Most published works on biodegradable materials have not been specifically focused on the mechanical performance and hence, the fracture behavior of these materials is generally disregarded (Tuba, Oláh, & Nagy, 2011).

Furthermore, the analysis of fracture surfaces represents an important issue to identify the different toughening mechanisms and the effect of different parameters on the composites fracture behavior (Cotterell, Chia, & Hbaieb, 2007). For experimental studies, the fractal and multifractal theories have been successfully applied to describe morphology of fracture surfaces by variation of the characteristic parameters of the multifractal spectra (Liu et al., 2009; Pérez, Bernal, & Piacquadio, 2012; Tarafder, Das, Chattoraj, Nasipuri, & Tarafder, 2010; Venkatesh, Chen, & Bhole, 2008; Zhang, Bai, Li, Chen, & Shen, 2011).

The aim of this investigation was to determine the effect of different types of nanoclay on the quasi-static fracture behavior of a commercial starch/PCL blend (MaterBi-Z). Some theoretical and experimental analyses were applied to study the fracture behavior observed for the different composites investigated.

2. Experimental

2.1. Materials

A commercial starch/PCL blend (called MaterBi-Z) kindly supplied by Novamont, Italy, was used as the matrix of the composites. It consists of 18 wt% starch, 75 wt% polycaprolactone (the main component) and 7 wt% additives.

Three different clays were used: one unmodified and two modified. The organoclays are prepared by modification of natural montmorillonite clays with different quaternary ammonium salts (Table 1), named Cloisite Na^+ (MMT), Cloisite 30B (C30B) and Cloisite 10A (C10A) purchased from Southern Clay Products Inc., USA. The reinforcements were employed as received. Their characteristics were first reported elsewhere (Pérez & Alvarez, 2008) Pristine montmorillonite (MMT) is hydrophilic while the modified clays (C30B and C10A) are more hydrophobic, being the second one (C10A) more hydrophobic than the first one (C30B).

2.2. Composites preparation

Composites with different clay contents (1, 2.5, 5 and 7.5 wt%) were prepared in an intensive Brabender type mixer with two counter-rotating roller rotors at 150 rpm and 100 °C for 10 min. After mixing, composite films with a nominal thickness of 0.4 mm were compression molded in a hydraulic press for 10 min at 100 °C under a pressure of 4.9 MPa.

2.3. Materials characterization

2.3.1. Fracture tests

Quasi-static fracture tests were carried out on deeply double edge-notched specimens (DENT), mode I (Fig. 1). The specimens were tested in a universal testing machine Interactive 10 K at 1 mm/min. Sample dimensions were: length (L) = 50 mm, width (W) = 20 mm and thickness (B) ≈ 0.4 mm. Distance between grips was 30 mm. Two properly aligned sharp notches of 5 mm were introduced by sliding a fresh razor blade into machined slots with the help of a specially designed device. The J-integral approach represents an extension of Linear Elastic Fracture Mechanics applied for not too ductile materials. In the last decades, the J-integral single-specimen formulation has been extensively applied in order to analyze ductile fracture of polymers (Bernal, Rink, & Frontini, 1999; Plati & Williams, 1975). In addition, the standard ASTM E 1820 allows to obtain a single point toughness value J_c to characterize quasi-brittle failure behavior (load–displacement curves with a sharp load drop at the point of fracture). J_c was calculated for the investigated composites based on the whole area under the load–displacement curve (U_{tot}) as follows:

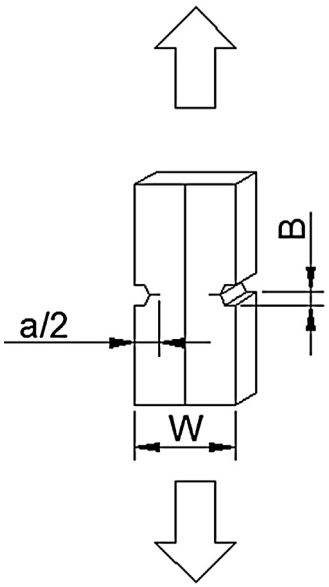

Fig. 1. Schematic showing a deeply double edge-notched specimen (DENT) considered for fracture tests.

$$J_c = \frac{\eta U_{tot}}{B(W-a)} \quad (1)$$

where U_{tot} is the overall fracture energy, B is the thickness, W is the width, a is the notch length and η is a geometrical factor defined by Grellmann and Reincke (2004):

$$\eta = -0.06 + 5.99\left(\frac{a}{W}\right) - 7.42\left(\frac{a}{W}\right)^2 + 3.29\left(\frac{a}{W}\right)^3 \quad (2)$$

All fracture tests were performed at room temperature. A minimum of five replicates were tested for each system and the average values with their deviations were reported.

2.4. Fracture surface analysis

Fracture surfaces of specimens broken in fracture tests were analyzed by scanning electron microscopy (SEM) after they had been coated with a thin layer of gold.

2.5. Multifractal analysis

Multifractal spectra were obtained by the box-counting method with the aim to analyze the fracture surfaces topography. First, SEM images were reduced to eliminate marks and then a global image for each material was obtained. The images were divided in many

Table 1
Characteristic of the used clays.

Material	Organic modifier	Modifier concentration (meq/100 g clay)	Specific gravity (g/cm^3)
MMT	None	–	2.86
C30B	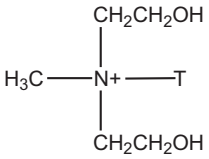	90	1.98
C10A	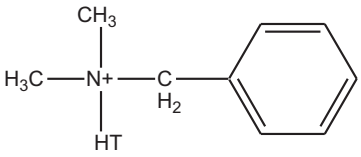	125	1.90

boxes of length $\varepsilon = 1/2$, 1/4, 1/6, 1/12, 1/15 and 1/25. The measure considered was:

$$u_{ij}(\varepsilon) = \frac{n_{ij}}{\sum n_{ij}} \tag{3}$$

where n_{ij} represents the mean gray value of the box i, j and $u_{ij}(\varepsilon)$ its probability which can be described by a multifractal spectrum $(\alpha, f(\alpha))$ as:

$$u_{ij}(\varepsilon) \propto \varepsilon^{\alpha} \tag{4}$$

$$N_{\alpha}(\varepsilon) \propto \varepsilon^{-f(\alpha)} \tag{5}$$

The number of boxes (N_{α}) with the same α-concentration represents the log/log version of a measure per unit of length:

$$\alpha(\varepsilon) = \frac{\log(u_{ij}(\varepsilon))}{\log(\varepsilon)} \tag{6}$$

The fractal dimension of each α-concentration is plotted by the spectrum $f(\alpha)$:

$$f(\alpha) = \frac{\log(N_{\alpha})}{\log(\varepsilon)} \tag{7}$$

More detailed information about the multifractal theory and its application for fracture surfaces analysis can be found in the literature (Liu et al., 2009; Pérez et al., 2012; Zhang et al., 2011). Experimental calculations of multifractal spectra were performed by the algorithm previously reported by Pérez (2013).

2.6. Fracture toughness modeling

The dependence of the composite fracture toughness with composition was theoretically analyzed by the model developed by Pukánszky and Maurer (1995). The proposed model considers the properties and content of the matrix and the matrix–filler interaction, as the major factors to determine the fracture toughness of composite materials. Plastic deformation of the matrix is recognized as the main toughening mechanism, initiated after voiding (Cotterell et al., 2007; Pukánszky & Maurer, 1995):

$$G_c = \frac{G_{c0}}{E/E_0}\frac{1-\varphi}{1+2.5\varphi}\exp(B\varphi) \tag{8}$$

where φ is the filler volume fraction, G_c and E are the fracture energy and elastic modulus of the composite material (subscript 0 corresponds to the matrix), respectively. The parameter B is related to the matrix–filler interaction of each system and it can be calculated by a reduced form of Eq. (8) as follows:

$$\ln(G_{\text{cred}}) = \ln\left(\frac{G_{c0}}{E_0/E}\frac{1+2.5\varphi}{1-\varphi}\right) = \ln(G_{c0}) + B\varphi \tag{9}$$

In addition, the plot of $\ln(G_{\text{cred}})$ should be linearly dependent on the composition with a slope of B to confirm the validity of the model. Any deviation from a linear regression allows estimating the presence of some structural effects, such as filler aggregation.

3. Results and discussion

3.1. Fracture behavior

Fig. 2a–c shows typical normalized load–displacement records obtained in fracture tests for the composites with MMT, C30B and C10A, respectively. Load values were normalized by the cross-section of the tested sample $(B^*(W-a))$ in order to account for differences in specimen thickness. In Fig. 2a–c the stable and unstable crack propagation were indicated with an arrow and a cross, respectively.

As it can be observed in Fig. 2a–c, most composites exhibited non-linear quasi-brittle fracture behavior characterized by the presence of unstable crack growth before maximum load or near this value. However, the composites with 1 or 2.5 wt% C30B displayed a higher amount of stable crack propagation followed by a precipitous drop of load to zero at a certain point after the maximum. Significantly higher displacement levels were also observed in these samples.

As all materials exhibited non-linear fracture behavior until maximum load and unstable crack growth at a certain point in the load–displacement curve, J-integral parameter at instability (J_c) was adopted to characterize the materials fracture behavior (Cotterell et al., 2007). J_c parameter values are presented in Fig. 2d along with their deviations. It can be observed in this figure, that the fillers used differently influenced the fracture response of the starch/PCL blend. MMT and C10A did not significantly affect the

Table 2
Multifractal spectra parameters for the MaterBi-Z matrix and its composites with C30B.

Material	$\alpha_{\min}$	$\alpha_{\max}$	$\Delta\alpha$	$f(\alpha_{\min})$	$f(\alpha_{\max})$	$\Delta f(\alpha)$
MBZ	1.8905	2.1746	0.2841	0.8855	0.256	0.6295
MBZ–2.5 wt% C30B	1.8198	2.2134	0.3936	0.7186	0.5943	0.1243
MBZ–7.5 wt% C30B	1.8988	2.1071	0.2083	0.8114	0.00	0.8114

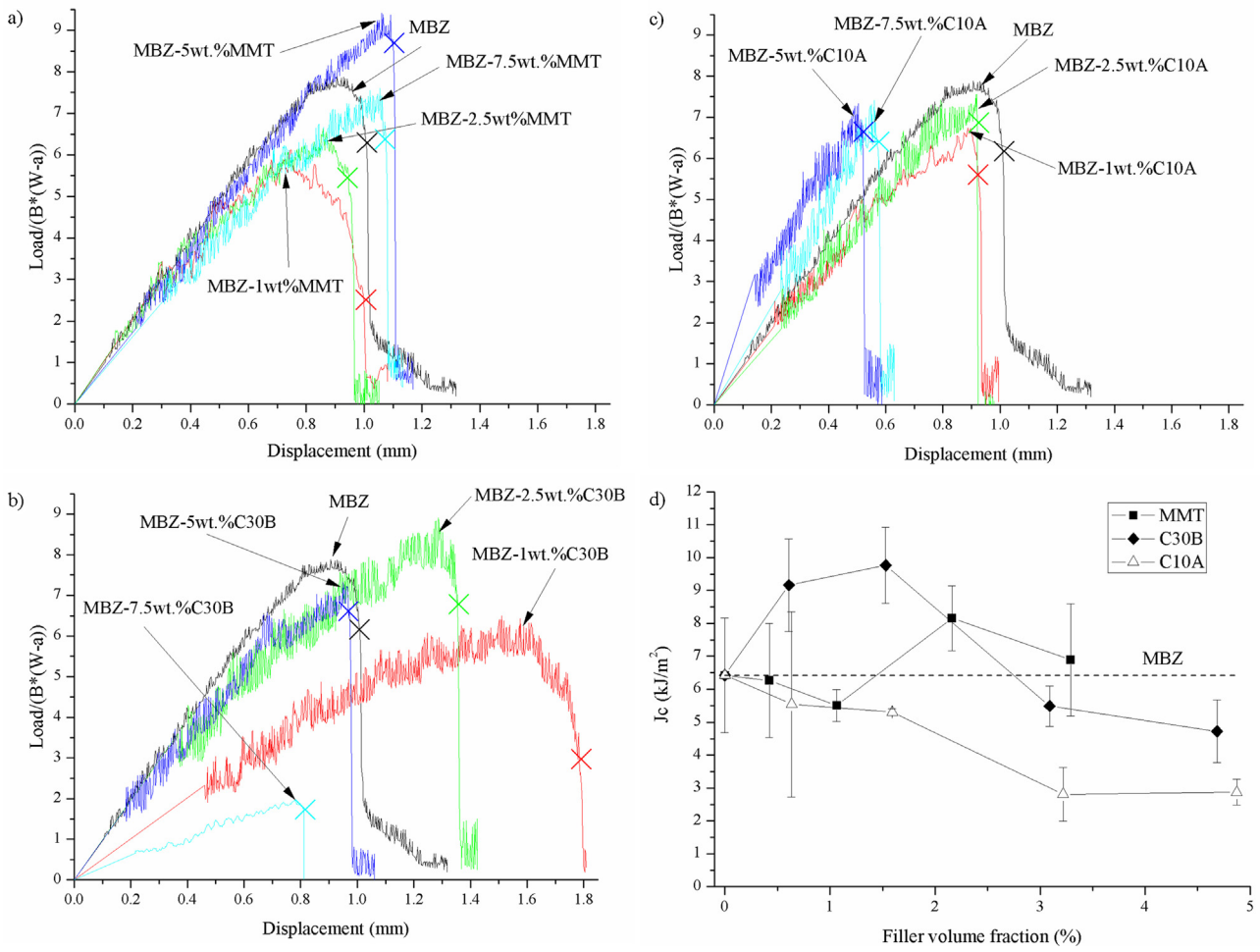

Fig. 2. Typical normalized load–displacement curves for the different composites investigated: (a) Composites with MMT. (b) Composites with C30B. (c) Composites with C10A and (d) *J*-integral parameter at instability (J_c) values.

material fracture toughness up to 2.5 wt% of filler (1.06 and 1.6 vol% of filler, respectively). Then, further increase in clay content was beneficial and detrimental to the J_c value in the case of MMT and C10A, respectively. Small amounts of C30B (1 and 2.5 wt%, 0.6 and 1.5 vol%, respectively), on the other hand, led to significant improvements in the material fracture toughness but amounts of clay higher than 5 wt% (3.1 vol%) led to slightly reduced J_c values respect to the matrix.

The dispersion of the different types of clay in MaterBi-Z obtained from X-ray diffraction analysis has been previously reported in another investigation (Pérez et al., 2007). In the case of the composites with MMT and C10A, the position of the (0 0 1) peak shifted to lower angles indicating that the polymer chains were intercalated into the clay platelets. On the other hand, although the peak is weaker, it remained at the same position for the composite with C30B which suggest that no polymer intercalation took place in this case (Pérez et al., 2007).

Regarding tensile properties, the composites with C10A displayed the highest values of Young's modulus and tensile strength among the three kind of fillers investigated as a result of their higher compatibility with the hydrophobic matrix. The observed differences in the dispersion of modified clays, and reflected in tensile properties, was the result of the organic group of each modifier. The benzyl group, present in C10A, has the largest surface area producing a strong interaction with the polymer matrix. In addition, the hydroxy-ethyl group of C30B has hydroxyl (OH) groups which are not highly compatible with the hydrophobic matrix, conducting to lower interaction allowing the debonding process. On the other hand, the intermediate values of tensile stiffness and strength for the MaterBi-Z/MMT composites could be probably related to a better filler/matrix interphase as it has been reported (Pérez et al., 2007).

The observed fracture behavior for the different composites is in agreement with previously reported tensile results. The composites with C30B which had initial intermediate compatibility with the starch/PCL blend but the worst dispersion among the three nanoclays investigated, displayed the best fracture behavior as a result of the matrix ductile tearing favored by filler-induced voiding, as it will be shown later. On the other hand, the composites with C10A and MMT showed the lowest and intermediate values of the J_c parameter, respectively.

3.2. Fracture surface analysis

SEM fractographs of the DENT specimens broken in fracture tests at different magnifications are shown in Figs. 3–6 for the starch/PCL blend matrix and the composites with 2.5 wt% of MMT, C30B and C10A, respectively.

Fig. 3 shows generalized ductile tearing of the starch/PCL blend matrix. The composite with MMT (Fig. 4) displays ductile tearing in a similar way to the matrix. Composite with 2.5 wt% of C30B (Fig. 5) also exhibit, as the matrix, generalized ductile tearing. This composite tends to induce even larger plastic deformation than neat matrix in accordance with the corresponding load–displacement curves.

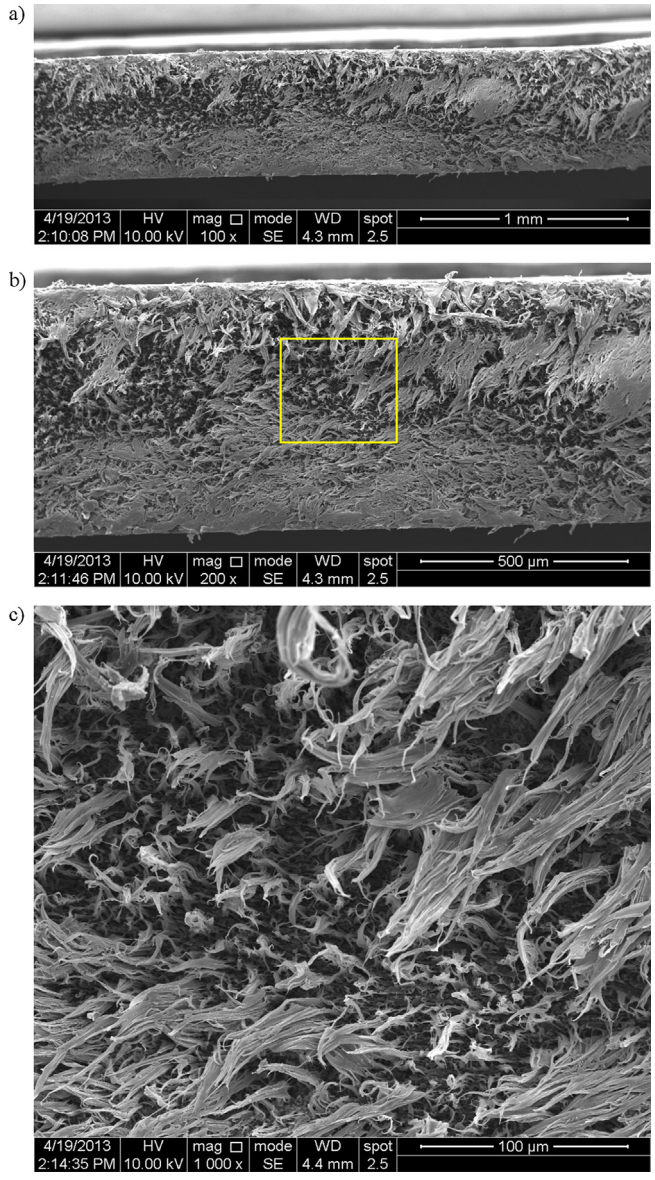

Fig. 3. Typical SEM fractograph of a DENT specimen of the MaterBi-Z matrix at different magnifications: (a) 100×, (b) 200× and (c) 1000×.

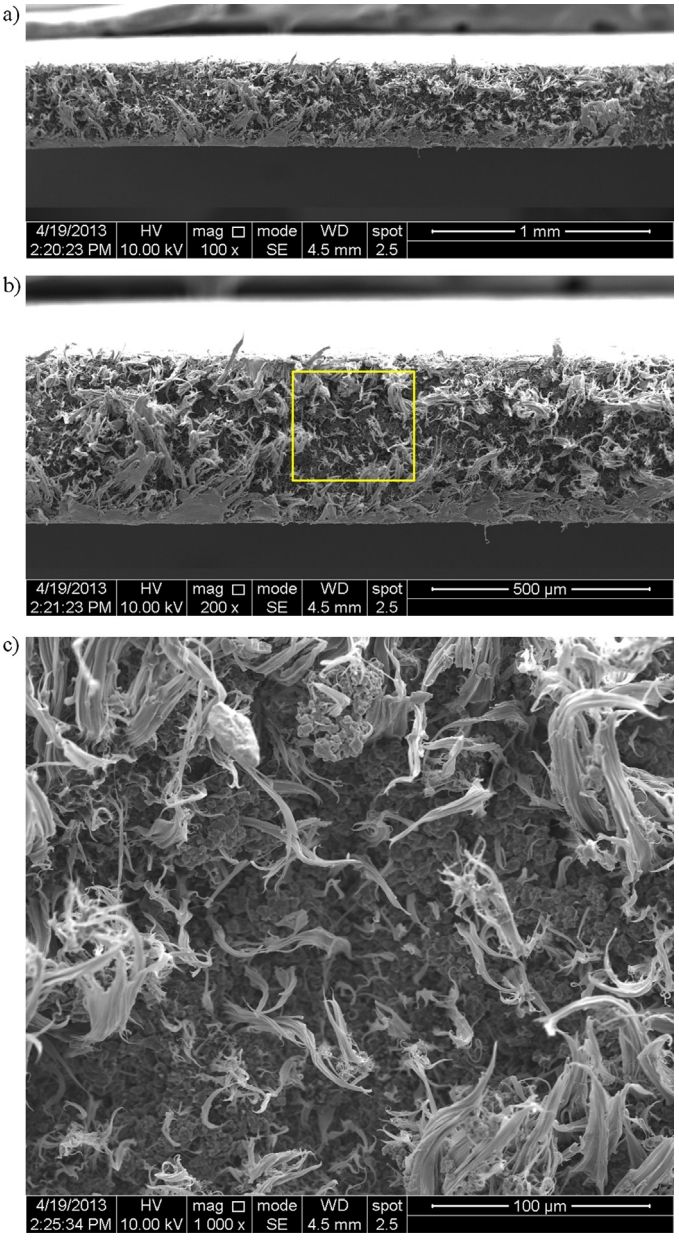

Fig. 4. Typical SEM fractograph of a DENT specimen of the composite with 2.5 wt% of MMT at different magnifications: (a) 100×, (b) 200× and (c) 1000×.

The composite with C10A (Fig. 6) displays regions with significantly different topographies. It can be observed zones of localized matrix ductile tearing whereas other regions exhibit smooth surfaces. These different kinds of topography are related to ductile and brittle fracture mechanisms, respectively. Their presence is in correspondence with the low fracture toughness displayed by this composite.

It can be recognized a really complex topography for all of the analyzed systems. Especially, the voids necessary to activate ductile tearing of the matrix were not clearly observed possibly due to the large plastic deformation of the matrix.

3.3. Multifractal analysis of topography

As the composites with C30B clay displayed the largest variations in fracture toughness, the multifractal theory was applied for these composites with the aim to correlate the fracture surfaces topography with the characteristic parameters spectra. The contents of C30B which correspond to the minimum and the maximum fracture toughness values (2.5 and 7.5 wt%, respectively) and the matrix were considered for the following analysis.

In order to apply the multifractal theory for experimental results the $\log N(\varepsilon)$ vs $\log(\varepsilon)$ curve should exhibit a linear regression, called the scaling range (Malcai, Lidar, & Biham, 1997). Based on the fact that data in Fig. 7a could be linearly fitted, multifractal theory was applied to study the fracture surfaces of starch/PCL blend. Similar scaling ranges were reported in the literature for fracture surfaces analysis (Malcai et al., 1997). The corresponding curves for the other composites analyzed were also linearly fitted (not shown here).

Multifractal spectra for starch/PCL blend and its composites with C30B are plotted in Fig. 7b (presented in Table 2). The results clearly show that shape and width ($\Delta\alpha$) of the spectra are different. The width of the curve increases for the composite with 2.5 wt% of C30B and decreases with increased filler content. These variations suggest that the fracture surfaces tend to be more irregular with the initial incorporation of C30B and more regular with increased content of clay (Zhang et al., 2011). It should be pointed out that the

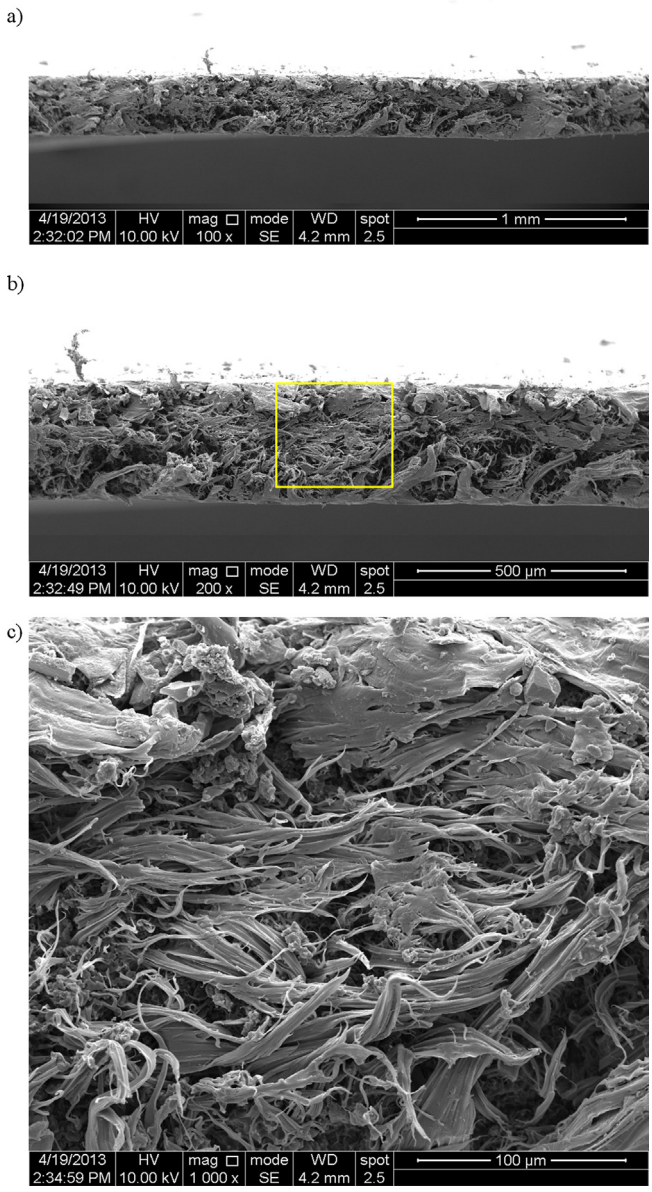

Fig. 5. Typical SEM fractograph of a DENT specimen of the composite with 2.5 wt% of C30B at different magnifications: (a) 100×, (b) 200× and (c) 1000×.

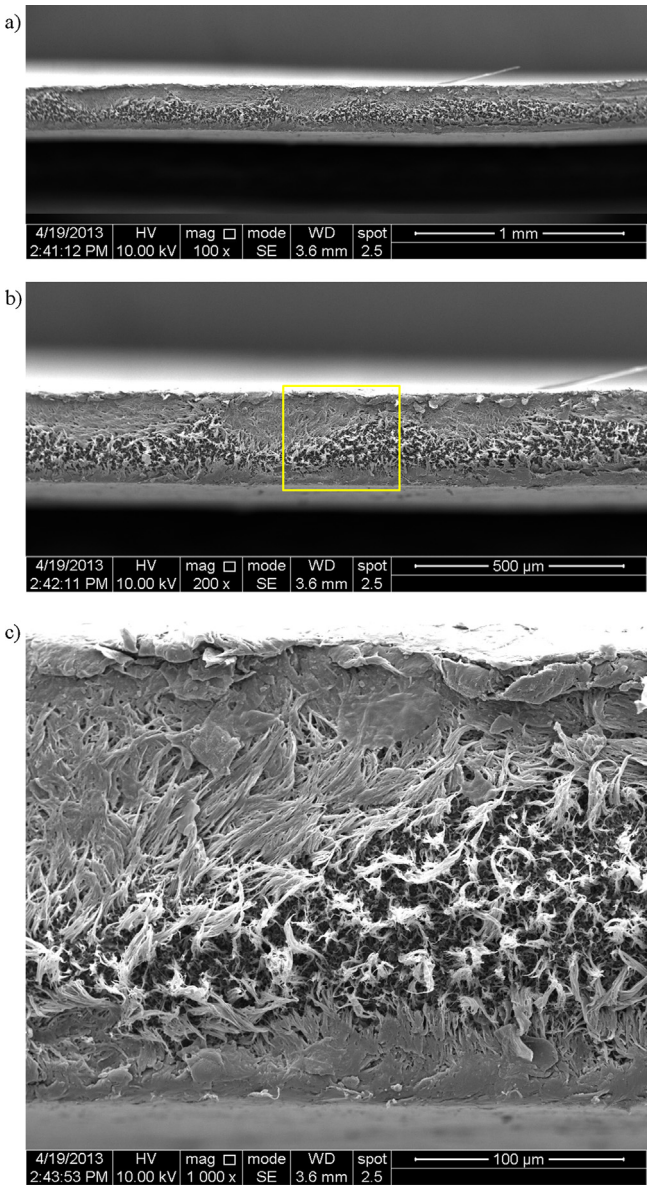

Fig. 6. Typical SEM fractograph of a DENT specimen of the composite with 2.5 wt% of C10A at different magnifications: (a) 100×, (b) 200× and (c) 1000×.

presence of brittle and ductile mechanisms is related to more regular or irregular surfaces, respectively. Described multifractal results can be qualitatively confirmed analyzing SEM micrographs. Fig. 7c shows the variation of $\Delta\alpha$ with the content of C30B. It can be seen similar variations for $\Delta\alpha$ and fracture toughness of the composites. Moreover, observed topographical variations were detected by the mean gray value distribution. Hence, the trend of fracture toughness observed with C30B content was also confirmed from the results of multifractal analysis.

3.4. Modeling of fracture toughness

The dependence of fracture toughness with filler content for the different composites was analyzed with the model proposed by Pukánszky and Maurer (1995). The obtained results are plotted in Fig. 8.

For all nanoclays considered, a linear regression for low filler contents was found. On the other hand, deviation from a linear fitting is achieved at large clay content suggesting the presence of some structural effect, probably clay agglomerates. Therefore, the model proposed by Pukánszky and Maurer can be applied for low clay contents.

The lowest value of the B parameter was obtained for the composites with C10A (Fig. 8), indicating a strong interfacial interaction between matrix and filler in this case. In contrast, the highest value corresponds to the composite with C30B which has the weakest filler–matrix interaction. An intermediate value of B was found for the composite with MMT suggesting that although it had the lowest initial compatibility with the matrix, a better interphase existed between this filler and the blend of plasticized starch and PCL within the composites, as mentioned before. The results obtained from the application of Pukánszky and Maurer model are in good agreement with the analysis of fracture surfaces.

It was established in the literature that surface modification of nanoclays can facilitate their exfoliation, normally considered as the best way to activate the filler effect. The potential toughening mechanisms for nanoclays are based on their large surface area to volume ratio and are assumed to be related to debonding for

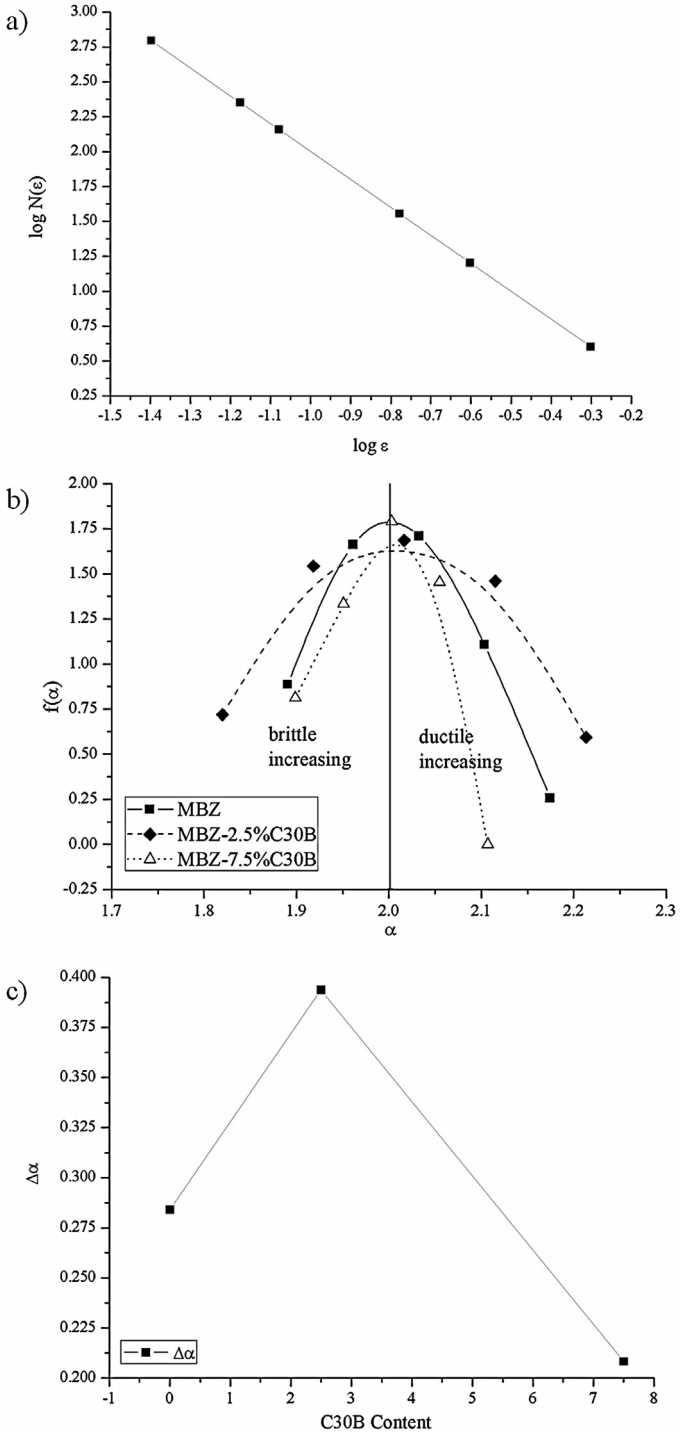

Fig. 7. Multifractal analysis of the fracture surfaces: (a) linear regression of $\log N(\varepsilon)$ vs $\log \varepsilon$ curve, (b) multifractal spectra for the MaterBi-Z matrix and the composites with C30B and (c) variation of the width $\Delta\alpha$ with C30B content.

exfoliated nanoclays or to splitting for intercalated ones. It should be pointed out that increased toughness was reported with not well exfoliated nanoclays. In addition, to activate the toughening mechanisms, voids are necessary to initiate crazes but the structure or chemistry of nanoclays can inhibit multiple crazing of the polymer matrix (Cotterell et al., 2007).

The composites with C10A exhibited the strongest filler–matrix interaction among the analyzed materials which would have hindered the voids formation necessary to promote multiple crazing of the polymer matrix leading to more brittle composites. This

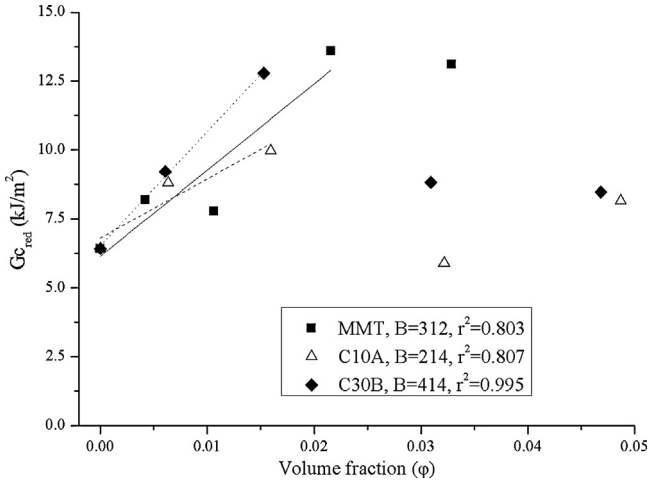

Fig. 8. Fracture toughness values as a function of filler volume fraction for the different MaterBi-Z composites.

behavior was in accordance with fracture surface observations. In addition, for larger filler contents clay agglomerates were detected, as it was previously discussed, which could be considered as critical-size flaws (Cotterell et al., 2007). Hence, these agglomerates would have contributed also to the embrittlement observed in the composites with C10A.

The toughening effect of C30B, in contrast, can be related to easy debonding of clay due to the low compatibility between this filler and the matrix. This assumption is in agreement with fracture surface analysis, where intensive ductile tearing was observed for composites with C30B for filler contents lower than 5 wt%. The presence of agglomerates was detected at large filler contents. Hence, a maximum was observed for fracture toughness a certain value of filler fraction in this composite.

Composites with MMT have not shown any significant toughening effect independently of filler content. Based on the intermediate value of interfacial interaction in this case, it can be suggested that the voiding necessary to initiate crazes could not be fully developed and hence, no significant toughening was achieved for these composites.

Finally, in the different composites investigated variations in fracture toughness values related to the filler type and content can be observed. These changes could be explained in terms of two counteracting effects: the debonding process for a weak filler–matrix interaction, leading to subsequent matrix plastic deformation (increased toughness), and the presence of agglomerates. The increase in filler content induced larger filler agglomerates which were detrimental to the materials fracture behavior. Filler agglomeration could be confirmed from deviations from a linear fitting in the model of Pukánszky and Maurer for the dependence of fracture toughness with composition.

4. Conclusions

The fracture behavior of composites based on starch/PCL blend reinforced with different clays was investigated. The complex fracture process could be successfully described by experimental and theoretical tools.

An improvement in the fracture behavior for the composites with low contents of C30B was obtained, probably due to the debonding of clay easily achieved from a low filler–matrix interaction. On the other hand, a strong interaction (MaterBi-Z/C10A) was detrimental to the composite fracture toughness. Intermediate values of fracture toughness were exhibited by the composites with

MMT as a result of its intermediate interaction with the plasticized starch/PCL matrix.

The results obtained for the fracture toughness were in good agreement with tensile results previously reported for the same composites.

From the results obtained here, it can be concluded that it is possible to modify the fracture properties of biodegradable composites based on plasticized starch/PCL blends reinforced with clay taking into account its further applications.

Acknowledgments

The authors want to thank the National Research Council of Argentina (CONICET) and the ANPCyT for financial support of this investigation and the Mechanics Groups of INTI for the developing of microscopic studies.

References

Bernal, C., Rink, M., & Frontini, P. M. (1999). Load separation principle in *J–R*. Curve determination of ductile polymers: Suitability of different material deformation functions used in the normalization method. *Macromolecular Symposia*, *147*, 235–248.

Chen, B., & Evans, J. R. G. (2005). Thermoplastic starch–clay nanocomposites and their characteristics. *Carbohydrate Polymers*, *61*, 455–463.

Corradini, E., Marconcini, J. M., Agnelli, J. A. M., & Mattoso, H. C. L. (2011). Thermoplastic blends of corn gluten meal/starch (CGM/starch) and corn gluten meal/polyvinyl alcohol and corn gluten meal/poly(hydroxybutyrate-co-hydroxyvalerate) (CGM/PHB-V). *Carbohydrate Polymers*, *83*, 959–965.

Cotterell, B., Chia, J. Y. H., & Hbaieb, K. (2007). Fracture mechanisms and fracture toughness in semi crystalline polymer nanocomposites. *Engineering Fracture Mechanics*, *74*, 1054–1078.

Davis, G. A., & Song, J. H. (2006). Biodegradable packaging based on raw materials from crops and their impact on waste management. *Industrial Crops and Products*, *23*, 147–161.

Godbole, S., Gote, S., Latkar, M., & Chakrabarti, T. (2003). Preparation and characterization of biodegradable poly-3-hydroxybutyrate–starch blend films. *Bioresource Technology*, *86*, 33–37.

Grellmann, W., & Reincke, K. (2004). Quality improvement of elastomers. Use of instrumented notched tensile-impact testing for assesment of toughness. *Materialprüfung*, *46*, 168–175.

Ishiaku, U. S., Pang, K. W., Lee, W. S., & Ishak, Z. A. M. (2002). Mechanical properties and enzymatic degradation of thermoplastic and granular sago starch filled poly(ε-caprolactone). *European Polymer Journal*, *38*, 393–401.

Liu, C., Jiang, X. L., Liu, T., Zhao, L., Zhou, W. X., & Yuan, W. K. (2009). Multifractal analysis of the fracture surfaces of foamed polypropylene/polyethylene blends. *Applied Surface Science*, *255*, 4239–4245.

Malcai, O., Lidar, D. A., & Biham, O. (1997). Scaling range and cutoffs in empirical fractals. *Physical Review E*, *56*, 2817–2828.

Pérez, E. (2013). Multifractal spectra obtained by the box-counting method – MATLAB™ codes. *Fractals*, submitted.

Pérez, C. J., & Alvarez, V. A. (2008). Isothermal crystallization of layered silicate/starch–polycaprolactone blend nanocomposites. *Journal of Thermal Analysis and Calorimetry*, *91*, 749–757.

Pérez, C. J., Alvarez, V. A., Stefani, P. M., & Vázquez, A. (2006). Non-Isothermal crystallization of MaterBi-Z/Clay nanocomposites. *Journal of Thermal Analysis and Calorimetry*, *88*, 825–832.

Pérez, C. J., Alvarez, V. A., Mondragón, I., & Vázquez, A. (2007). Mechanical Properties of layered silicate/starch–polycaprolactone blend nanocomposites. *Polymer International*, *56*, 686–693.

Pérez, C. J., Alvarez, V. A., & Vázquez, A. (2008). Creep behavior of layered silicate/starch–polycaprolactone blends nanocomposites. *Materials Science and Engineering A*, *480*, 259–265.

Pérez, C. J., Alvarez, V. A., Mondragón, I., & Vázquez, A. (2008). Water uptake behavior of layered silicate/starch–polycaprolactone blend nanocomposites. *Polymer International*, *57*, 247–253.

Pérez, E., Bernal, C., & Piacquadio, M. (2012). Multifractal analysis of tensile toughness and filler dispersion for polypropylene–$CaCO_3$ composites. *Applied Surface Science*, *258*, 8940–8945.

Plati, E., & Williams, J. G. (1975). The determination of the fracture parameters for polymers in impact. *Polymer Engineering Science*, *15*, 470–477.

Pukánszky, B., & Maurer, F. H. (1995). Composition dependence of the fracture toughness of heterogeneous polymer systems. *Polymer*, *36*, 1617–1625.

Reis, K. C., Pereira, J., Smith, A. C., Carvalho, C. W. P., Wellner, N., & Yakimets, I. (2008). Characterization of polyhydroxybutyrate–hydroxyvalerate (PHB-HV)/maize starch blend films. *Journal of Food Engineering*, *89*, 361–369.

Rosa, D. S., Lopes, D. R., & Calil, M. R. (2005). Thermal properties and enzymatic degradation of blends of poly(3-caprolactone) with starches. *Polymer Testing*, *24*, 756–761.

Scott, G. (2000). 'Green' polymers. *Polymer Degradation and Stability*, *68*, 1–7.

Siracusa, V., Rocculi, P., Romani, S., & Dalla Rosa, M. (2008). Biodegradable polymers for food packaging: A review. *Trends in Food Science & Technology*, *19*(12), 634–643.

Sorrentino, A., Gorrasi, G., & Vittoria, V. (2007). Potential perspectives of bionanocomposites for food packaging applications. *Trends in Food Science & Technology*, *18*, 84–95.

Tarafder, M., Das, S. K., Chattoraj, I., Nasipuri, M., & Tarafder, S. (2010). Fractal-based quantification of crack paths for determination of effective microstructural length scales and fracture toughnes. *Scripta Materialia*, *62*, 109–112.

Tuba, F., Oláh, L., & Nagy, P. (2011). Characterization of reactively compatibilized poly(D,L-lactide)/poly(e-caprolactone) biodegradable blends by essential work of fracture method. *Engineering Fracture Mechanics*, *78*, 3123–3133.

Venkatesh, B., Chen, D. L., & Bhole, S. D. (2008). Three-dimensional fractal analysis of fracture surfaces in a titanium alloy for biomedical applications. *Scripta Materialia*, *59*, 391–394.

Vertuccio, L., Gorrasi, G., & Sorrentino, A. (2009). Nano clay reinforced PCL/starch blends obtained by high energy ball milling. *Carbohydrate Polymers*, *75*, 172–179.

Wu, C. S. (2003). Physical properties and biodegradability of maleated-polycaprolactone/starch composite. *Polymer Degradation and Stability*, *80*, 127–134.

Xu, J., Li, R. K. Y., Heng, Y. Z., & Mai, Y. W. (2006). Biodegradable poly(propylene carbonate)/montmorillonite nanocomposites prepared by direct melt intercalation. *Materials Research Bulletin*, *41*, 244–252.

Zhang, Q. X., Yu, Z. Z., Xie, X. L., Naito, K., & Kagawa, Y. (2007). Preparation and crystalline morphology of biodegradable starch/clay nanocomposites. *Polymer*, *48*, 7193–7200.

Zhang, Y. H., Bai, B. F., Li, J. Q., Chen, J. B., & Shen, C. Y. (2011). Multifractal analysis of the tensile fracture morphology of polyvinylidene chloride/glass fiber composite. *Applied Surface Science*, *257*, 2984–2989.